Supplementary Information

Title: A novel amelogenesis-inspired hydrogel composite for remineralization of enamel non-cavitated lesions.

Keywords: amelogenin-derived peptide; bioactive glass; hydrogel; non-cavitated lesions; remineralization

2. Materials and methods

2.1 Materials

QP5 and QP5 labelled with fluorescein isothiocyanate isomer (FITC) were synthesized by Ontores Biotechnologies (Zhejiang, China). The 58S BG, composed of SiO_2-CaO-P_2O_5 with an average particle size of 30 μm, was purchased from Kunshan Chinese Technology New Materials CO, LTD (Jiangsu, China). Hydroxyethyl cellulose (HEC) was from Tokyo Kasei Industrial CO., LTD. (Tokyo, Japan), and the viscosity of its 2% aqueous solution at 25 ℃ was 6500mPa.s. Potassium citrate tribasic monhydrate (MW=324.42, AR) was from Chengdu Cologne Chemical CO., LTD. (Chengdu, China). Glycerol (MW=92.09, AR) and Sorbitol (MW=182.18, AR) were obtained from Shanghai Macklin Biochemical CO., LTD. (Shanghai, China). The calcium and phosphorus assay kits were from Nanjing Jiancheng Bioengineering Institute (C004-2, C006-1, Jiancheng, Nanjing, China) and cell counting kit-8 was from DOJINDO (CK04, Dojindo, Kumamoto, Japan). Sodium azide was purchased from Shanghai Chemical Reagent Factory (Shanghai, China). The acid-resistant nail varnish was from Maybelline (New York, USA). Unless otherwise stated, other chemicals were purchased from Sigma-Aldrich (St. Louis, MO, US) and were used as received.

2.2 Preparation of BQ hydrogel composite

2.2.1 Characterization of QP5 and BG

QP5 (QPYQPVQPHQPMQPQTKREEVD) was synthesized by Ontores Biotechnologies via standard Fmoc solid-phase chemistry. The integrity and structure of QP5 were confirmed by reverse-phase high-performance liquid chromatography (RP-HPLC; CHTH Sci and Tech, Beijing, China), electrospray ionization mass spectrometry (ESI-MS; Shimadzu, Kyoto, Japan) and circular dichroism (CD) spectroscopy (J-1500, JASCO, Tokyo, Japan). The morphology and composition of BG were measured by scanning

electronic microscopy (SEM; Inspect F50; FEI, USA), energy dispersive spectroscopy (EDS; INCA350, Oxford, UK) and X-ray photoelectron spectroscopy (XPS; Ultra DLD, Kratos, UK).

2.2.2 Screening of hydrogel matrix concentration

The appearance, viscosity, fluidity and stability were comprehensively used as evaluation indicators to screen out the matrix concentration suitable for clinical use and for the subsequent formulation optimization. Briefly, HEC of different weight was added to 300 mL deionized water (DIW) under constant temperature (25 °C, 1000 rpm). After the HEC particles were fully swollen, potassium citrate was added to promote the cross-linking of HEC to form hydrogels with the mass percentage of HEC at 0.5 wt%、1.0 wt%、1.5 wt%、2.0 wt%、2.5 wt% and 3.0 wt%. The hydrogels were macroscopically observed whether delaminated, precipitated and liquefied[1]. NDJ-9S digital display rotational viscometer (Grows Instrument, Shanghai, China) was used to measure the viscosity of the hydrogels at 6 rpm using a No. 4 rotor, and each sample was measured three times in parallel. In addition, the fluidity of the hydrogels was evaluated by the tilting test tube method[2]. About 5 mL of each hydrogel sample was placed in a test tube (Φ1.5 cm; length: 18 cm) with a flow distance of 15 cm. Then the test tube was rapidly tilted to 20° to the horizontal plane and the time for the hydrogel reaching the lip of the test tube was measured.

2.2.3 Orthogonal experimental design and preparation of BQ hydrogel composite

In order to explore the optimal ingredient ratio of HEC/potassium citrate/glycerol/sorbitol, which has the moderate viscosity and the maximum mineral ions release capacity, an orthogonal optimization experiment was designed in which the concentration of HEC and potassium citrate and the ratio of glycerol to sorbitol were taken as investigation factors and the appearance, stability, viscosity, fluidity, pH and calcium and phosphorus release were comprehensively used as indicators (Table S1). The appearance, stability, viscosity and fluidity were tested as described above in section 2.2.2 and pH of the hydrogel was determined by dissolving 100 mg of it in 100 mL of DIW. Test for ion releasing capacity of the 9 hydrogels were carried out

according to method of section 2.4.2. Each sample was measured three times in parallel. In this study, a three-variable, three-level values matrix was constructed. The orthogonal design, which led to an optimized combination (formulation 3) through 9 runs, was showed in Table S3 and Figure S3.

Table S1. The Orthogonal Experimental Design (3 Levels and 3 Factors)

Level	Factor		
	HEC %(w/v) (A)	**glycerol: sorbitol (B)**	**potassium citrate %(w/v) (C)**
1	1.5	3:1	0.5
2	2.0	1:1	1
3	2.5	1:3	2

1 mol/L sorbitol solution was prepared by progressively adding a certain amount of sorbitol to DIW until complete dissolution. After filtering, the sorbitol was mixed with glycerol at a ratio of 3:1 and the mixture was continuous stirred for 30 minutes until clear for later use. First, 1.5 (w/v) HEC was dispersed in DIW at 25 °C under constant magnetic stirring (1000 rpm) for 20 minutes. After that, an equal volume of the mixture of sorbitol and glycerol was added dropwise to HEC solution under constant conditions (25 °C, 1000 rpm), following with the addition of QP5 to make its final concentration of 25 μmol/L[3]. The obtained solution was continous stirred until the HEC particles swelled and the system was gradually clarified. Then, BG (5% w/w or 10% w/w) and potassium citrate were added and continue to stir to form the BQ (5% or 10%) hydrogel in situ. A series of hydrogels, BG (5% or 10%) hydrogel, QP5 hydrogel and HEC hydrogel were obtained by the same method. The prepared hydrogels were stored at 4°C for further use.

2.3 Characterization of BQ hydrogel composite

2.3.1 Morphology observation

The morphology of hydrogels was observed by SEM (Inspect F50; FEI, USA) with 20 kV accelerated voltage. Before scanning, hydrogels were quickly frozen in -80°C and then

freeze-dried. The freeze-dried samples were sputtered with gold under vacuum to ensure the conductivity.

2.3.2 Fourier transform infrared spectroscopy analysis

The fourier transform infrared (FTIR, NICOLET iS10, Thermo Scientific, Friars Drive Hudson, NH, USA) spectra was measured in the wavenumber ranging from 400 to 4000 cm^{-1}[4, 5].

2.3.3 Cytotoxicity

The cytotoxicity test was carried out in accordance to ISO 10993-5. Briefly, samples of 10% BQ hydrogel composite were immersed in Dulbecco's Modified Eagle Medium (DMEM; GE Healthcare, USA) containing 5% fetal bovine serum (FBS; GE Healthcare, USA) at a ratio of 0.2 g/mL for 24 h at 37 °C, and the supernatant was collected to prepare the material extracts of a series of concentrations of 10% to 100%[6]. The extracts were co-cultured with human gingival fibroblasts for 24h and the cell viability was measured by the CCK-8 assay.

2.3.4 Water loss rate

According to the reported method, 1g hydrogel samples were placed in 2mL centrifuge tubes and then were dried in an oven (DHG-9070A, keelrein, Shanghai, China) at 37 °C. The samples were weighed continuously for 50 days to calculate the water loss rate[5].

2.3.5 Rheology

The rheological properties were measured on an HR-20 Discovery rheometer (TA Instrument, New Castle, DE, USA) with a 40 mm parallel plate at 25 °C. A dynamic frequency sweep measurement in the range of 0.1-100 rad/s at a fixed strain amplitude (λ = 0.1%) was applied for the storage modulus G' and loss modulus G"[5, 7].

2.4 Capacity of enamel binding, ions releasing and pH buffering of BQ hydrogel

2.4.1 Test for QP5 binding capacity

Four kinds of hydrogels were prepared under dark conditions, including FITC hydrogel, The fluorescein isothiocyanate (FITC)-labeled QP5 hydrogel, BQ (FITC-QP5) hydrogel and HEC hydrogel. The 100 μm thick enamel samples (and samples etched for 45 s by 37% phosphoric acid) were treated with these four kinds of hydrogels and were

observed by confocal laser scanning microscope (CLSM; OLYMPUS, Tokyo, Japan)[8, 9].

2.4.2 Test for ion releasing capacity

2 mL hydrogel was immersed in 15 mL centrifuge tubes containing 3 mL of HEPES (pH 7.4), and the samples were incubated at 37 °C under continuous shaking at 100 rpm. The supernatant was withdrawn to detect the cumulative release of calcium and phosphorus at different time points (10, 15, 20, 25, 30, 60, 120, 240, 480 min) and then replaced by new N-2-hydroxyethylpiperazine-N-2-ethane sulfonic acid (HEPES) solution. The content of calcium and phosphorus was determined by phosphomolybdic acid method and methyl thymol blue colorimetry[9, 10].

2.4.3 Test for pH buffering capacity

2 mL hydrogel was immersed in 15 mL centrifuge tubes containing 3 mL of artificial saliva (pH 4.0) which composed of 20 mM HEPES, 0.9 mM KH_2PO_4, 1.5 mM $CaCl_2$, 130 mM KCl and 1 mM NaN_3, and the samples were incubated at 37 °C under continuous shaking at 100 rpm[11, 12]. The pH value at different time points (0 min, 30 min and 120 min) was measured. The characterization of the pH was performed with a Mettler Toledo™ FiveEasy™ F20 pH/mV Meter (METTLER TOLEDO, Swiss).

2.5 Remineralizing effect of BQ hydrogel composite on enamel NCLs *in vitro*

2.5.1 Enamel sample preparation

Sound bovine incisors free of caries and cracks were selected, and the crowns were separated from the roots using a low-speed diamond saw (Struers Minitom; Struers, Copenhagen, Denmark) under running water. Enamel blocks were then embedded in epoxy resin. The labial surfaces were polished with 1000-, 1500-, 2000-, 2500- and 5000- grit silicon carbide discs. All the samples were coated with two layers of acid-resistant nail vanish, leaving a 5×4 mm or 5×5 mm window for subsequent treatment. The baseline surface microhardness (SMH_0) was measured by a Vickers hardness tester (MMT-X7A, Matsuzawa, Japan) under a load of 50 g for 10 s[13]. Enamel samples with SMH_0 between 300~400 VHN were included in the study.

2.5.2 Lesion formation

Demineralization was carried out by immersing enamel blocks in demineralization solution composed of 50 mM acetic acid (pH 4.5), 2.2 mM KH_2PO_4, 2.2 mM Ca $(NO_3)_2$,

5.0 mM NaN_3 and 0.5 ppm NaF for 3 days at 37 ℃ with continuous low-speed magnetic stirring (100 rpm/min)[14]. Afterwards, the surface microhardness (SMH1) was measured by the same method used to determine SMH_0 as described in 2.5.1. Next, the exposed surfaces of partial samples were half-covered with acid-resistantnail varnish for following treatments (Fig.1).

2.5.3 Remineralization in artificial saliva

All the demineralized specimens were assigned to seven groups: enamel treated with 1) 5% BG hydrogel; 2) 10% BG hydrogel; 3) 5% BQ hydrogel; 4) 10% BQ hydrogel; 5) 25 μmol/L QP5 hydrogel; 6) sodium fluoride (NaF) varnish (Duraphat, Colgate Palmolive, USA); and 7) HEC hydrogel. The demineralized area of enamel blocks was applied with 40 μL of the above hydrogels respectively at 25℃ for 30 min. The fluoride varnish was carefully removed using a surgical blade and cotton swabs soaked in 50% acetone solution, and then the samples were immersed in artificial saliva (as described in 2.4.2, pH 7.0) at 37 ℃ for 1 week with a change of solution each day[15, 16]. Next, the exposed surfaces of partial samples were half-covered with acid-resistantnail varnish for following treatments (Fig.1).

2.5.4 Microhardness measurement

The surface microhardness after treatment (SMH_2) was measured again as previously described in 2.5.1. The percentage recovery of surface microhardness (%SMHR) was calculated according to the following equation[17]: $\%SMHR= (SMH_2-SMH_1)/(SMH_0-SMH_1) \times 100\%$.

2.5.5 SEM observation of enamel surface after remineralization

After remineralization, the enamel samples were sonicated for 15 min and rinsed with deionized water. The surface of the sample was sputtered with Au and observed via SEM (Inspect F50; FEI, USA).

2.5.6 Transverse microradiography (TMR) analysis

Enamel slabs were cross sectioned into slices approximately 1 mm thick containing demineralized and remineralized region. The slices were then polished to produce enamel slices of 100 μm thickness[18]. The samples were then exposed alongside an

aluminium calibration step-wedge to a monochromatic CuK X-ray source (Philips, Eindhoven, Netherlands) operating at 20 kV and 20 mA for 30 min[19]. The lesion depth (LD), mineral loss (ΔZ) and mineral content (MC) at selected depths were analyzed with imaging software (Transversal Microradiography Software 2006, Inspektor Research Systems BV). The change of lesion depth and mineral loss was calculated by the following equations[20]: Mineral Gain ($\Delta\Delta Z$) = $\Delta Z_d - \Delta Z_r$, Lesion depth reduction (ΔL) = $L_d - L_r$, where ΔZ_d is mineral content variation before and after demineralization, ΔZ_r is mineral content variation before and after remineralization, L_d is lesion depth after demineralization, and L_r is lesion depth after remineralization.

2.5.7 XRD analysis of enamel after remineralization

The X-ray diffraction patterns of the remineralized samples were recorded with a diffractometer of Cu Kα radiation at 1.54 Å with a scanning rate of 0.02°/step in the 2θ range from10° to 60°.

2.5.8 Color assessment

A colorimeter (Vita Easyshade Advance 4.0, VITA, Germany) was used to assess the color change which could give the $L^*a^*b^*$ values represented the dimensions of color space as prescribed by the CIELAB color system. Each enamel sample was measured three times before and after demineralization and after remineralization. A standard light source box fixed with D65 light was used to standardize the ambient environment during the test. The colorimeter was calibrated with a calibration block before measurement under the same conditions. The color change (ΔE) between two measurements were calculated using the following equation[21]: $\Delta E = [(\Delta L^*)^2 + (\Delta a^*)^2 + (\Delta b^*)^2]^{1/2}$. The enamel surface color recovery ratio (%CRR): $\%CRR = \Delta E_1/\Delta E_0 \times 100\%$, where ΔE_0 is the color change before and after demineralization, and ΔE_1 is the color change before and after remineralization.

2.5.9 Performance evaluation of the remineralized layer

The samples after remineralization were placed in the above demineralization solution (as described in 2.5.2, pH 4.5) for 5 h. Mineral calcium (Ca) or phosphorus (P) concentrations before and after immersion were measured by phosphomolybdic acid method and methyl thymol blue colorimetry and Ca/P loss was expressed as

μg/mm^{222}. All samples were submitted to a 5-day de- and remineralization cycle. Erosion was performed using citric acid (0.3%, pH 2.6, 4 times a day for 10 min). Following, the blocks were submitted to treatment with no-fluoride dentifrice（Colgate clean classic, Colgate-Palmolive Company1, China） slurry for 15 s[23-25]. Surface loss was determined by scanning the surface of each block from the remineralized surfaces across the wear surfaces by profilometry (MarSurf CD120, Germany). The mean value of 5 readings was calculated for each block.

2.6 *In vivo* remineralization effect and biosafety of BQ hydrogel composite

2.6.1 SD rat caries model and sample collection

The animal experiment was performed with a modified rat caries model[26]. 50 male specific-pathogen-free, 19-day-old Sprague-Dawley (SD) rats were purchased from Sichuan Dashuo Biological Co., Ltd. and then they were determined to be free of endogenous S. *mutans* infection. The rats were then infected orally with S. *mutans* UA159 for three days and were randomly assigned into 5 groups[26, 27]: 10% BQ hydrogel, 10% BG hydrogel, QP5 hydrogel, NaF varnish and HEC hydrogel group. They were treated topically using a brush for 5 min three times daily for 5 weeks and were fed the Keyes 2000 diet (Trophic, Nantong, China) and 5% sucrose water[27]. All rats were weighed weekly and their physical state was recorded. Then the rats were euthanized by CO_2 asphyxiation and the jaws were surgically removed.

2.6.2 Micro-computed tomography (Micro-CT) analysis

Mandibles were scanned at a 7 μm isotropic voxel resolution using the Scanco Medical μCT 50 (Scanco Medical AG, Brüttisellen, Switzerland). The 3D images were reconstructed using Scanco Evaluation software v. 1.1.11.0 (Scanco Medical AG) and were color coded by setting the spectral range from -998.8 to 1999.8 so as to provide a mineral map of the lesions and render an enhanced visualization. The resultant color-coded images illustrated the distribution of mineral density within the lesion and different parts of the tooth. The color closer to red indicated a higher density, while the color closer to blue indicated a lower density[28]. Mineral density and residual molar enamel volume of molar areas were measured using Evaluation software (Scanco)[29].

2.6.3 Oral mucosa stimulation experiment

Seven-week-old male Syrian hamsters were purchased from Liaoning Changsheng Biotechnology Co., Ltd. The material was soaked with a cotton ball with a diameter of about 10 mm until saturated, and the one soaked with normal saline was used as control. After anesthesia, these cotton balls were placed in the cheek pouch for 30 min. All treated cheek pouch mucosae were subjected to macroscopic examination after treatment and the histologic examination was performed after 24h according to the ISO 10993-10, Annex B.3[30].

2.6.4 Hemolysis test

The diluted anticoagulant blood was prepared as described in previous study[5]. 2.5 g hydrogel and 5 mL PBS were added to the 15 mL centrifuge tube and incubated at 37 ℃ for 30 min. Then 0.1 mL diluted hemocyte was added and incubated together with the hydrogel for another hour. The absorbance of the supernatant was determined at 540 nm. The blood samples were mixed with deionized water and PBS as positive control and negative control, respectively. A specific formula was used to calculate the hemolysis rate (%): Hemolysis Rate (%) = ($OD_{hydrogel} - OD_{negative}$)/ ($OD_{positive} - OD_{negative}$) ×100%

2.7 Statistical analysis

Statistical analyses were performed using GraphPad Prism 9.0.0 (GraphPad Software Inc.). All results were expressed as means ± SD (Standard deviation of the mean). Statistical significance was determined using the one-way analysis of variance (ANOVA) and Tukey's multiple comparison tests at a p-value of 0.05. The normality and homogeneity of all data were checked by the Kolmogorov–Smirnov test and Levene test, respectively.

Supplementary figures

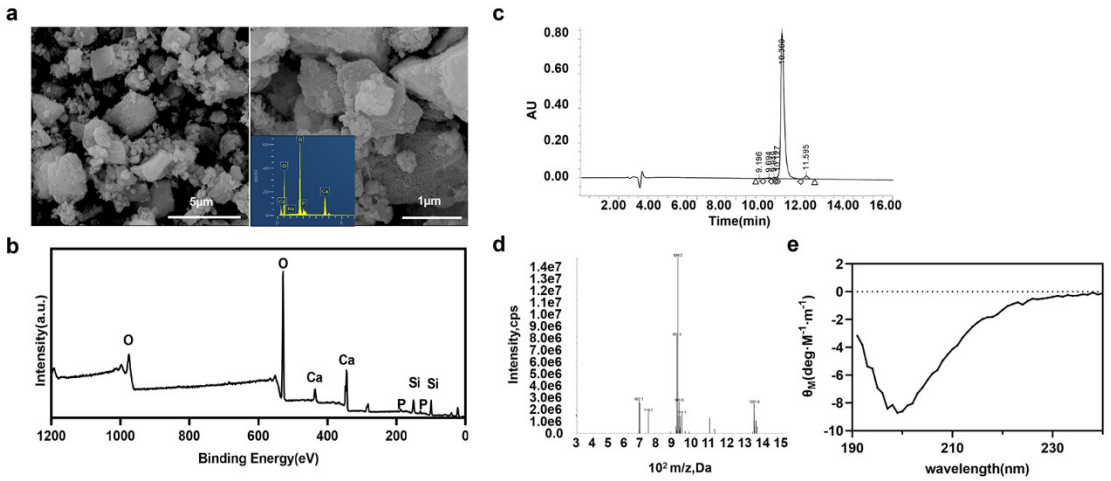

Figure S1. Characterization of BG and QP5. (a) High-resolution SEM images of BG powder at 20,000x and 80,000x magnification and the corresponding EDS x-ray maps of Ca/P/Si/O of BG. (b) XPS spectra of BG. Identification of the structure and purity of QP5 by HPLC (c) and ESI-MS (d). (e) CD spectra of QP5 with representative secondary structures.

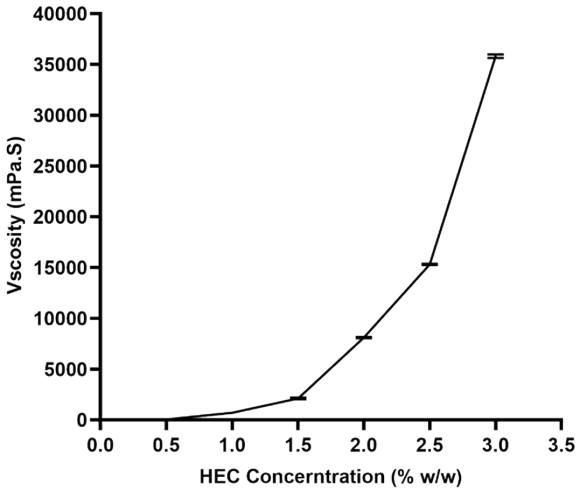

Figure S2. Curve of viscosity of HEC aqueous solution varying with HEC concentration. Data of different points of concerntration are presented as the mean ± SD (n=3).

TABLE S2. Physical properties of hydrogels with different HEC concentration

HEC	appearance	viscosity	liquidity	stability
0.5%	clear and transparent	-	+++	stable
1.0%	clear and transparent	+	+++	stable
1.5%	clear and transparent	++	++	stable
2.0%	clear and transparent	++	++	stable
2.5%	yellowish lear transparent	+++	+	stable
3.0%	yellowish lear transparent	+++	-	stable

Viscosity: Extremely low (-); Low (+); Moderate (++); High (+++)

Liquidity: Extremely low (-); Low (+); Moderate (++); High (+++)

Table S3. Combination of Variables of the Orthogonal Experimental Design for BQ hydrogel Preparation [9 Runs (3 Levels and 3 Factors)]

Formulation	Factors			viscosity	liquidity	pH
	A	B	C			
1	1	1	1	4520±28	1’18’’ ±4’’	10.48±0.02
2	1	2	2	3488±12	54’’ ±2’’	10.59±0.00
3	1	3	3	2158±24	41’’ ±2’’	10.69±0.00
4	2	1	2	7177±13	4’37’’ ±5’’	10.73±0.01
5	2	2	3	7074±41	3’51’’ ±5’’	10.82±0.00
6	2	3	1	6554±135	4’43’’ ±12’’	10.76±0.00
7	3	1	3	18792±90	17’53’’ ±17’’	10.78±0.00
8	3	2	1	15983±4	11’49’’ ±11’’	10.94±0.00
9	3	3		11197±157	8’6’’ ±6’’	10.78±0.00

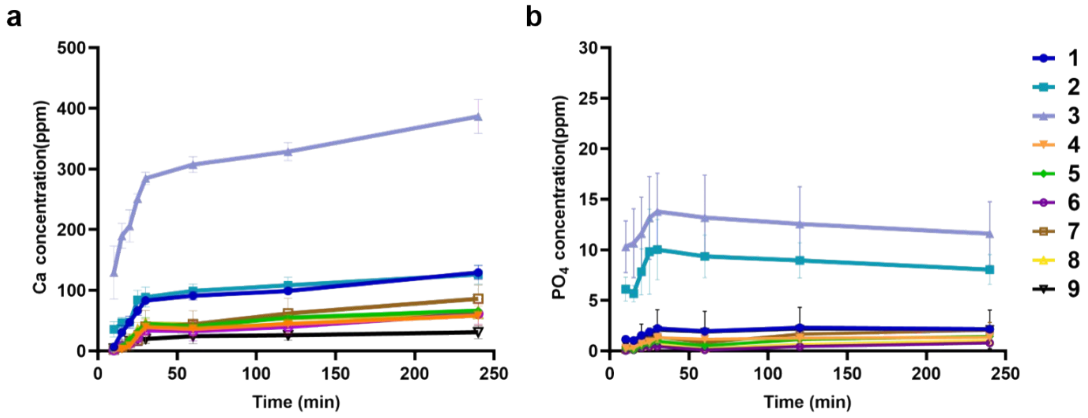

Figure S3. Calcium (a) and phosphorus (b) ions release from the 9 orthogonal designed formulations. Data of different points of time are presented as the mean ± SD (n=3).

References

1. L. Binder, J. Mazal, R. Petz, V. Klang and C. Valenta, *Skin Res Technol*, 2019, **25**, 725-734.
2. Y. Sato, T. Oba, N. Natori and K. Danjo, *Chem Pharm Bull*, 2010, **58**, 1582-1586.
3. D. Li, X. Lv, H. Tu, X. Zhou, H. Yu and L. Zhang, *Front Mater Sci*, 2015, **9**, 293-302.
4. L. Liu, H. Wen, Z. Rao, C. Zhu, M. Liu, L. Min, L. Fan and S. Tao, *Int J Biol Macromol*, 2018, **108**, 376-382.
5. Y. Huang, F. Shi, L. Wang, Y. Yang, B. M. Khan, K. L. Cheong and Y. Liu, *Int J Biol Macromol*, 2019, **132**, 729-737.
6. Y. Chen, Y. Zhou, S. Yang, J. J. Li, X. Li, Y. Ma, Y. Hou, N. Jiang, C. Xu and S. Zhang, *Mater Sci Eng C-Mater*, 2016, **66**, 84-91.
7. H. Lee, B. Rukmanikrishnan and J. Lee, *Int J Biol Macromol*, 2019, **141**, 538-544.
8. L. Ding, S. Han, K. Wang, S. Zheng, W. Zheng, X. Peng, Y. Niu, W. Li and L. Zhang, *Regen Biomater*, 2020, **7**, 283-292.
9. Y. Wang, D. Hu, J. Cui, Y. Zeng, X. Gan, Z. Chen, Q. Ren and L. Zhang, *J Mater Chem B*, 2020, **8**, 10373-10383.
10. Q. Cai, C. Qiao, J. Ning, X. Ding, H. Wang and Y. Zhou, *Chem Res Chinese U*, 2019, **35**, 908-915.
11. N. A. Al-eesa, F. S. L. Wong, A. Johal and R. G. Hill, *Dent Mater*, 2017, **33**, 1324-1329.
12. D. Wu, J. Yang, J. Li, L. Chen, B. Tang, X. Chen, W. Wu and J. Li, *Biomaterials*, 2013, **34**, 5036-5047.
13. H. Milly, F. Festy, M. Andiappan, T. F. Watson, I. Thompson and A. Banerjee, *Dent Mater*, 2015, **31**, 522-533.

14. Y. Yang, X. P. Lv, W. Shi, J. Y. Li, D. X. Li, X. D. Zhou and L. L. Zhang, *J Dent Res*, 2014, **93**, 520-524.
15. S. N. Mohd Said, M. Ekambaram and C. K. Yiu, *Int J Paediatr Dent*, 2017, **27**, 163-173.
16. K. Wang, X. Wang, H. Li, S. Zheng, Q. Ren, Y. Wang, Y. Niu, W. Li, X. Zhou and L. Zhang, *RSC advances*, 2018, **8**, 1647-1655.
17. J. A. Cury, G. S. Simoes, A. A. Del Bel Cury, N. C. Goncalves and C. P. Tabchoury, *Caries Res*, 2005, **39**, 255-257.
18. M. Fan, M. Zhang, H. H. K. Xu, S. Tao, Z. Yu, J. Yang, H. Yuan, X. Zhou, K. Liang and J. Li, *Dent mater*, 2020, **36**, 210-220.
19. S. E. Langhorst, J. N. O'Donnell and D. Skrtic, *Dent Mater*, 2009, **25**, 884-891.
20. L. P. Comar, B. M. Souza, J. Martins, M. G. Santos, M. A. R. Buzalaf and A. C. Magalhaes, *J Dent*, 2017, **63**, 81-84.
21. F. Hua, J. Yan, S. Zhao, H. Yang and H. He, *Clin Oral Investig*, 2020, **24**, 2079-2089.
22. L. Zhou, H. M. Wong, Y. Y. Zhang and Q. L. Li, *ACS Appl Mater Interfaces*, 2020, **12**, 3021-3031.
23. M. J. Moretto, A. C. Delbem, M. M. Manarelli, J. P. Pessan and C. C. Martinhon, *J Dent*, 2013, **41**, 1302-1306.
24. C. M. Alencar, M. E. S. Ribeiro, J. F. Zaniboni, T. P. Leandrin, A. M. Silva and E. A. Campos, *Braz Dent J*, 2022, **33**, 68-76.
25. I. D. Rochel, J. G. Souza, T. C. Silva, A. Pereira, D. Rios, M. Buzalaf and A. C. Magalhães, J Oral Sci, 2011, **53**, 163-168.
26. S. Han, Y. Fan, Z. Zhou, H. Tu, D. Li, X. Lv, L. Ding and L. Zhang, *Arch Oral Biol*, 2017, **73**, 66-71.
27. W. Jiang, Y. Wang, J. Luo, X. Chen, Y. Zeng, X. Li, Z. Feng and L. Zhang, *Appl Environ Microbiol*, 2020, **86**, e00527-20.
28. M. Shahmoradi and M. V. Swain, *J Dent*, 2016, **46**, 23-29.
29. B. He, S. Huang, J. Jing and Y. Hao, *Arch Oral Biol*, 2010, **55**, 134-141.
30. Y. Niwano, K. Konno, T. Matayoshi, K. Nakamura, T. Kanno and K. Sasaki, *Regul Toxicol Pharmacol*, 2017, **90**, 206-213.